



Technical Report
RAL-TR-97-032

The Quasi-Fixed MSSM

B C Allanach et al

July 1997

© Council for the Central Laboratory of the Research Councils 1997

Enquiries about copyright, reproduction and requests for additional copies of this report should be addressed to:

The Central Laboratory of the Research Councils
Library and Information Services
Rutherford Appleton Laboratory
Chilton
Didcot
Oxfordshire
OX11 0QX
Tel: 01235 445384 Fax: 01235 446403
E-mail library@rl.ac.uk

ISSN 1358-6254

Neither the Council nor the Laboratory accept any responsibility for loss or damage arising from the use of information contained in any of their reports or in any communication about their tests or investigations.

The Quasi-Fixed MSSM

S.A. Abel^a and B.C. Allanach^b

^a *Service de Physique Théorique
Université Libre de Bruxelles
Bruxelles 1050, Belgium*¹

^b *Rutherford Appleton Laboratory
Chilton, Didcot OX11 0QX, England*

The infra-red fixed points are determined for the parameters of the MSSM. They dominate the renormalisation group running when the top-Yukawa is in the quasi-fixed point regime (i.e. large at the GUT scale). We examine this behaviour analytically, by solving the full set of one-loop renormalisation group equations in the approximation that the electroweak contributions are negligible, and also numerically. The parameters are significantly focused towards their fixed points at the weak scale, and the top-quark trilinear coupling A_t has a quasi-fixed point which predicts $A_t = -0.59m_g$ independently of the input parameters at the unification scale. This considerably increases the predictivity of the MSSM in this regime.

¹Address after 1st Sept 1997: Theory Division, CERN CH-1211, Geneva 23

1 Introduction

The renormalisation group running of parameters from high to low scales is often dominated by infra-red stable fixed points. Formally, these are points in parameter space where couplings are invariant under the renormalisation group. From any initial values at say the GUT scale, the couplings will flow asymptotically toward the infra-red fixed points at lower scales. In certain cases, a possible example being the top-quark Yukawa coupling, the convergence is enough to increase the predictivity of the theory [1, 2]. In the Minimal Supersymmetric Standard Model (MSSM) for instance, in the limit that one can neglect h_b, h_τ , the bottom and tau Yukawa couplings, a prediction for $h_t(m_t)$ yields a prediction for $\tan\beta$ through the relation

$$\sin\beta = \frac{m_t(m_t)}{vh_t(m_t)} \quad (1)$$

where $m_t(m_t) \sim 167 \text{ GeV}$ is the running top quark mass extracted from experiment and $v = 174.1 \text{ GeV}$ is the Higgs vacuum expectation value parameter extracted from M_Z . The MSSM fixed point prediction for h_t is $h_t(m_t) = \sqrt{7/18}g_3(m_t)$, where g_3 is the QCD gauge coupling. For $m_t(m_t) \approx 167 \text{ GeV}$, $\alpha_s(m_t) = 0.108$, we obtain the fixed point prediction $h_t(m_t) = 0.73$. Substituting these values into Eq.(1), however, yields $\sin\beta = 1.32$, and hence this is an unphysical scenario. There are then two possible scenarios within the MSSM:

- The assumption of small h_b, h_τ is not valid and therefore $\tan\beta$ is large, say $\tan\beta > 30$. This possibility was discussed in Ref.[3].
- The top quark Yukawa coupling is outside the domain of attraction of the fixed point but $\tan\beta < 30$ is small [2].

In this paper, we shall examine what happens in the second scenario. For larger values of $h_t(M_{GUT})$ a different type of behaviour takes over called quasi-fixed behaviour. Large values of $h_t(M_{GUT})$ quickly converge to the envelope bounding the perturbative region, giving a quasi-fixed point (QFP) prediction at m_t . The QFP limit is formally defined as the landau pole of h_t at the scale M_{GUT} . Although the renormalised top coupling is still running with scale Q it is insensitive to $h_t(M_{GUT})$. We define the quasi-fixed regime to be where $h_t(m_t)$ is close to the QFP prediction.

These fixed and quasi-fixed behaviours (with electroweak and two-loop contributions included and for a top mass of 140 GeV) are shown in figure (1), where we show a numerical running for the MSSM, with a superpotential of the form

$$W = h_U Q_L H_2 U_R + h_D Q_L H_1 D_R + h_E L H_1 E_R + \mu H_1 \epsilon H_2, \quad (2)$$

in which generation indices are implied, and the superfields have the standard definition [4]. The program described in Ref.[5, 6] is the one we use to perform the running (without thresholds). We also take $\alpha_s(m_t) = 0.108$ throughout, and define M_{GUT} to be the scale Q for which $\frac{3}{5}\alpha_1(Q) = \alpha_2(Q)$. We do not unify g_3 with g_2 and g_1 because g_3 at the high scale is sensitive to GUT threshold effects [7]. The fixed point is only slightly dependent on the electroweak corrections and the focusing behaviour is not changed significantly by them, although the numerical value of the QFP prediction is slightly modified.

For this reason we shall neglect electroweak corrections in later analytic discussions of focusing behaviour and find that, when they are switched off, all our numerical and analytic results are in good agreement. From figure (1), the quasi-fixed point prediction is $h_t(m_t) = 1.09$, so that for $m_t = 167$ GeV, we find $\tan \beta = 1.85$.

This focusing property of h_t is well known; our aim in this paper is to examine what happens to the other couplings, in particular the soft supersymmetry breaking parameters, when h_t is in the quasi-fixed regime. We now state our main conclusion: some of the soft supersymmetry breaking terms also have QFPs; in the quasi fixed regime, their low energy predictions are focused to running values which are independent of the inputs at M_{GUT} . These soft parameters formally have true fixed point values as well, but a necessary condition for the true fixed point predictions to be valid is that h_t is at its fixed point prediction, which we have shown above to be untrue for small $\tan \beta$ and so these values are not physically relevant. Some of the remaining couplings (which do not formally have QFPs) also have true fixed points, and they are significantly focused towards them. They might then be said to exhibit quasi-fixed behaviour even though they are not fully independent of the inputs at the GUT scale.

The parameter that, as we shall show, always has a QFP and that shows the most striking convergence is A_t , the trilinear stop coupling. Its running is shown in figure (2) for various starting values at the GUT scale. When h_t is in the quasi-fixed regime, this coupling is determined to be,

$$A_t(m_t) = -0.59 m_g. \quad (3)$$

(We use A_t as shorthand for $A_{U_{33}}$ and m_g for the gluino mass). In this and subsequent occasions where we demonstrate numerically the (lack of) dependence on the initial conditions, we take, simply for convenience, the supersymmetry breaking terms,

$$\begin{aligned} -\delta\mathcal{L} = & m_{ij}^2 z_i z_j^* + \frac{1}{2} M_A \lambda_A \lambda_A \\ & + A_U h_U \tilde{q}_L^* h_2 \tilde{u}_R + A_D h_D \tilde{q}_L^* h_1 \tilde{d}_R + A_E h_E \tilde{l}^* h_1 \tilde{e}_R + B\mu h_1 \epsilon h_2 + \text{h.c.}, \end{aligned} \quad (4)$$

to be of the ‘constrained’ MSSM (CMSSM) form at the GUT scale;

$$\begin{aligned} A_{U,D,E} &= A \\ m_{ij}^2 &= \delta_{ij} m_0^2 \\ M_A &= m_{1/2}. \end{aligned} \quad (5)$$

In Eq.(4), z_i stand for all scalar fields in the theory. We will specifically refer to $m_{Q_{ij}}^2$, $m_{U_{ij}}^2$, $m_{D_{ij}}^2$ for the left-handed squarks, the right-handed up and the right-handed down squark soft mass parameters respectively.

Later we shall show that the strong focusing seen in figure (2) is quite independent of the pattern of supersymmetry breaking. Hence, since both A_t and $\tan \beta$ are fully determined in the quasi-fixed regime, there are two less free parameters in *any* version of the MSSM. The mass spectrum of the CMSSM, for example, depends (to first order in m_b/m_t) only on m_0 and $m_{1/2}$.

The behaviour of A_t suggests that other low scale soft parameters may be quite insensitive to the high scale inputs and, as stated above, we shall indeed find this to be the case, by solving the renormalisation group equations (RGEs) analytically for all the soft supersymmetry breaking terms.

2 The fixed points

First, let us derive the fixed point values that the couplings would run towards in the infra-red if the top-quark fixed point were valid. They correspond to the point where the beta function vanishes for the coupling in question [1, 2]. So, for example, using the RGEs of Refs.[8] without electroweak or two-loop contributions,

$$\begin{aligned}\frac{dg_3}{dt} &= -3\frac{g_3^3}{16\pi^2} \\ \frac{dh_t}{dt} &= \frac{h_t}{16\pi^2}\left(6h_t^2 - \frac{16}{3}g_3^2\right),\end{aligned}\tag{6}$$

the RGE of h_t^2/g_3^2 [2] vanishes when

$$\frac{h_t^2}{g_3^2} = \frac{7}{18}.\tag{7}$$

In the evolution from high to low energy scales, h_t^2/g_3^2 runs towards this value because the fixed point is infra-red stable. A similar procedure can be carried out for all of the couplings in the MSSM, again neglecting electroweak corrections and all but the top Yukawa contributions to the running. If there are any large hierarchies in the soft masses (comparable in size to the hierarchy between the top and bottom Yukawa couplings) then this approximation may not always be valid. We will investigate this possibility in detail elsewhere [10]. Normalising the couplings by the gluino mass, so that $\tilde{A}_t \equiv A_t/m_g$, $\tilde{B}_t \equiv B/m_g$ and $\tilde{m}_i^2 \equiv m_i^2/m_g^2$, we find the following infra-red fixed points;

$$\begin{aligned}-\tilde{A}_U &= \begin{pmatrix} \frac{25}{18} & \frac{25}{18} & 1 \\ \frac{25}{18} & \frac{25}{18} & 1 \\ 1 & 1 & 1 \end{pmatrix} & -\tilde{A}_D &= \begin{pmatrix} \frac{16}{9} & \frac{16}{9} & \frac{16}{9} \\ \frac{16}{9} & \frac{16}{9} & \frac{16}{9} \\ \frac{89}{54} & \frac{89}{54} & \frac{89}{54} \end{pmatrix} \\ \tilde{m}_Q^2 &= \begin{pmatrix} \frac{8}{9} & 0 & 0 \\ 0 & \frac{8}{9} & 0 \\ 0 & 0 & \frac{41}{54} \end{pmatrix} & \tilde{m}_U^2 &= \begin{pmatrix} \frac{8}{9} & 0 & 0 \\ 0 & \frac{8}{9} & 0 \\ 0 & 0 & \frac{17}{27} \end{pmatrix} \\ \tilde{m}_D^2 &= \begin{pmatrix} \frac{8}{9} & 0 & 0 \\ 0 & \frac{8}{9} & 0 \\ 0 & 0 & \frac{8}{9} \end{pmatrix} & \tilde{m}_2^2 &= -\frac{7}{18} \\ & & \mu^2 &= 0 \\ & & \tilde{B} &= \frac{7}{18}.\end{aligned}\tag{8}$$

The parameter m_2^2 has a negative fixed point, because it is dragged down by the top Yukawa coupling. This guarantees electroweak symmetry breaking in the fixed regime, and underlies the breaking that is found away from it. Fixed points for a subset of Eq.(8) (\tilde{A}_t , μ , $\tilde{\mu}_2^2$, \tilde{m}_t^2 , \tilde{B} , $\tilde{m}_{Q_t}^2$) were previously found by Lanzagorta and Ross [2], and our results agree with those. Notice that the fixed points are independent of the quark basis in which we choose to calculate them (so long as it is still accurate to assume $h_t \approx h_{U_{33}}$ to be the dominant Yukawa coupling in that basis). (Note, however, that if we choose a basis where the down quarks' masses are diagonal at m_t , then $A_{D_{i \neq j}}$ is of course not defined at m_t whereas $A_{U_{i \neq j}}$ is, and vice versa.)

3 Exact one-loop RGE solutions

There is obviously a difference between the fixed point value of A_t , and that in Eq.(3). This is because Eq.(3) is in fact also a quasi-fixed point; even though it is focused, A_t is still running at m_t . Evidently we need to solve the renormalisation group equations and apply the solutions to the quasi-fixed regime. In this section we do this analytically and exactly to one loop and in the approximation that the electroweak and non- h_t Yukawa contributions are negligible. It is simplest to do this in terms of the ratio of strong coupling constants;

$$r(Q) \equiv \frac{\alpha_3(M_{GUT})}{\alpha_3(Q)} = 1 - 6 \alpha_3(M_{GUT}) \log\left(\frac{Q}{M_{GUT}}\right). \quad (9)$$

The RGE for $R \equiv h_t^2/g_3^2$ may be solved [2] such that

$$R(r) = \frac{7}{18 - 18 r^{7/9} + 7 r^{7/9} R_0^{-1}} \quad (10)$$

where $R_0 \equiv R(M_{GUT})$. The fixed point corresponds to $r \rightarrow 0$, and the QFP to $R_0 \rightarrow \infty$ with $r = 1/(25 \times 0.108) = 0.37$, so that $R(r) < R^{QFP}(r) = 0.72$. Next we solve for following combinations of couplings to find solutions in terms of \tilde{A}_t and $\tilde{m}_{U_{33}}^2$; here the suffix 0 again implies values taken at the GUT scale and $\alpha, \beta = 1, 2, 3$ and $i, j = 1, 2$

$$\begin{aligned} \tilde{B} - \frac{1}{2}\tilde{A}_t &= -\frac{8}{9}(r-1) + r(\tilde{B} - \frac{1}{2}\tilde{A}_t)|_0 \\ \tilde{A}_{D_{3\alpha}} - \frac{1}{6}\tilde{A}_t &= \frac{40}{27}(r-1) + r(\tilde{A}_{D_{3\alpha}} - \frac{1}{6}\tilde{A}_t)|_0 \\ \tilde{A}_{D_{i\alpha}} &= \frac{16}{9}(r-1) + r \tilde{A}_{D_{i\alpha}}|_0 \\ \tilde{A}_{U_{ij}} - \frac{1}{2}\tilde{A}_t &= \frac{8}{9}(r-1) + r(\tilde{A}_{U_{ij}} - \frac{1}{2}\tilde{A}_t)|_0 \\ \tilde{A}_{U_{3i}} - \tilde{A}_t &= r \left(\frac{R r^{7/9}}{R_0} \right)^{1/6} (\tilde{A}_{U_{3i}} - \tilde{A}_t)|_0 \\ \tilde{A}_{U_{i3}} - \tilde{A}_t &= r \left(\frac{R r^{7/9}}{R_0} \right)^{1/12} (\tilde{A}_{U_{i3}} - \tilde{A}_t)|_0 \\ \tilde{m}_1^2 &= r^2 \tilde{m}_1^2|_0 \\ \tilde{m}_2^2 - \frac{3}{2}\tilde{m}_{U_{33}}^2 &= -\frac{4}{3}(1-r^2) + r^2(\tilde{m}_2^2 - \frac{3}{2}\tilde{m}_{U_{33}}^2)|_0 \\ \tilde{m}_{Q_{33}}^2 - \frac{1}{2}\tilde{m}_{U_{33}}^2 &= \frac{4}{9}(1-r^2) + r^2(\tilde{m}_{Q_{33}}^2 - \frac{1}{2}\tilde{m}_{U_{33}}^2)|_0 \\ \tilde{m}_{Q_{ii}}^2 &= \frac{8}{9}(1-r^2) + r^2 \tilde{m}_{Q_{ii}}^2|_0 \end{aligned}$$

$$\begin{aligned}
\tilde{m}_{U_{ii}}^2 &= \frac{8}{9}(1-r^2) + r^2 \tilde{m}_{U_{ii}}^2|_0 \\
\tilde{m}_{D_{\alpha\alpha}}^2 &= \frac{8}{9}(1-r^2) + r^2 \tilde{m}_{D_{\alpha\alpha}}^2|_0 \\
\tilde{m}_{Q_{\alpha\beta}}^2 &= r^2 \left(\frac{R r^{7/9}}{R_0} \right)^{1/12} \tilde{m}_{Q_{\alpha\beta}}^2|_0 \quad \alpha\beta = i3 \text{ or } 3i \\
\tilde{m}_{U_{\alpha\beta}}^2 &= r^2 \left(\frac{R r^{7/9}}{R_0} \right)^{1/6} \tilde{m}_{U_{\alpha\beta}}^2|_0 \quad \alpha\beta = i3 \text{ or } 3i,
\end{aligned} \tag{11}$$

with the other off-diagonal squark mass squareds \tilde{m}_o^2 being

$$\tilde{m}_o^2 = r^2 \tilde{m}_o^2|_0. \tag{12}$$

We stress that these solutions are for generic couplings², and care should be taken over the choice of basis especially for the \tilde{A} -terms. One instance is the basis used in Ref.[6], where the down quarks are diagonal, and the up quark Yukawas are diagonalised just by a rotation by the CKM matrix on the left handed up quarks. In this basis, \tilde{A}_{3i} behaves more like \tilde{A}_{ij} because of the cancellation of certain terms in the RGE. Now we need to solve for \tilde{A}_t and $\tilde{m}_{U_{33}}^2$ themselves; the RGE for \tilde{A}_t becomes

$$r \frac{d\tilde{A}_t}{dr} = \frac{16}{9} + 2\tilde{A}_t R_t + \tilde{A}_t \tag{13}$$

and gives

$$\begin{aligned}
\tilde{A}_t &= \frac{18}{7} R \left(-1 + r^{7/9} \left(\frac{16}{9} - \frac{7}{9} r \right) \right) + \\
&\quad \left(\frac{R}{R_0} \right) r^{7/9} \left(r \tilde{A}_t|_0 - \frac{16}{9} (1-r) \right).
\end{aligned} \tag{14}$$

To solve for $\tilde{m}_{U_{33}}^2$, we form the RGE for $Z \equiv \tilde{m}_{U_{33}}^2 + \tilde{m}_{Q_{33}}^2 + \tilde{m}_2^2 - \tilde{A}_t^2$,

$$r \frac{dZ}{dr} = -\frac{32}{9} - \frac{32}{9} \tilde{A}_t + 2ZR + 2Z, \tag{15}$$

whose solution is

$$\begin{aligned}
Z &= \frac{32}{9} R r^{7/9} (1-r)^2 + \\
&\quad \frac{1}{9} \left(\frac{R}{R_0} \right) r^{7/9} \left(32 r (1-r) \tilde{A}_t|_0 + 9 r^2 Z|_0 - \frac{16}{9} (7-25r)(1-r) \right).
\end{aligned} \tag{16}$$

Substituting from Eq.(11) into Z gives,

$$\tilde{m}_{U_{33}}^2 - \frac{1}{3} \tilde{A}_t^2 - \frac{1}{3} Z = \frac{8}{27} (1-r^2) + \frac{1}{3} r^2 (2\tilde{m}_{U_{33}}^2 - \tilde{m}_{Q_{33}}^2 - \tilde{m}_2^2)|_0. \tag{17}$$

²Given the proviso of no large hierarchies in soft masses.

Eqs.(11,12,14,16,17) are exact solutions to the full set of one-loop RGEs when h_t and g_3 are dominant. The solutions for the third family squark masses were found in Ref.[11], where electroweak corrections were also included. However, this is to our knowledge, the first time the full set of solutions has appeared for all the parameters. Here we neglect electroweak corrections principally because they only serve to obscure the fixed point structure which is governed by h_t and g_3 .

We are now able to make some comments more specific to the MSSM in the quasi-fixed regime. Firstly note that, at the QFP ($R_0^{-1} = 0$), both \tilde{A}_t and Z are independent of *any* of the input parameters. This then is the reason for the remarkable convergence of \tilde{A}_t seen in figure (2) and is in fact true of $\tilde{A}_{U_{\alpha 3}}$ and $\tilde{A}_{U_{3\alpha}}$ although, generally, \tilde{A}_t converges most strongly. Because their leading terms are dependent only on r , it makes sense to refer to them as QFPs as well. Inserting $R = 0.72$ and $r = 0.37$ into Eq.(14), we find the quasi-fixed value for $\tilde{A}_{U_{\alpha 3}}$ and $\tilde{A}_{U_{3\alpha}}$ consistent with the numerical determination in Eq.(3);

$$\tilde{A}_{U_{\alpha 3}} = \tilde{A}_{U_{3\alpha}} = -0.58. \quad (18)$$

The remaining A parameters converge approximately linearly to their fixed point, and the m^2 terms quadratically to theirs. This dependence is due to the diverging gluino mass $m_g = r^{-1}m_g|_0$.

Coincidentally, in the constrained MSSM (CMSSM), there are a number of other QFPs which can be deduced from the solutions above, including one for $\tilde{m}_{U_{33}}^2$ itself (which is why we wrote Eq.(11) in terms of it). In our analytic approximation these are

$$\begin{aligned} \tilde{A}_{U_{\alpha 3}} = \tilde{A}_{U_{3\alpha}} &= -0.58 \\ \frac{6}{5}\tilde{A}_{D_{3\alpha}} - 2\tilde{A}_{U_{ij}} &= 0.46 \\ \tilde{A}_{D_{i\alpha}} - 2\tilde{A}_{U_{ij}} &= 0.58 \\ \tilde{m}_{U_{33}}^2 &= 0.53 \\ \tilde{m}_{Q_{33}}^2 + \tilde{m}_2^2 &= 0.28 \\ \tilde{m}_{Q_{ii}}^2 + 2\tilde{m}_2^2 &= 0.04 \\ \tilde{m}_{U_{ii}}^2 + 2\tilde{m}_2^2 &= 0.04 \\ \tilde{m}_{D_{\alpha\alpha}}^2 + 2\tilde{m}_2^2 &= 0.04 \\ \tilde{m}_1^2 + 2\tilde{m}_2^2 &= -0.73 \end{aligned} \quad (19)$$

where the meanings of the indices are as before. In the CMSSM, all of these combinations are independent of the GUT scale parameters when $R_0 \rightarrow \infty$, and converge to their QFPs roughly in the same manner as \tilde{A}_t . The value of R_0 regulates how quickly the convergence to the QFP occurs (with $R_0^{-1} = 0$ giving instant convergence). The running of $\tilde{m}_{U_{33}}^2$ for various starting values in the CMSSM is shown in figure (3), and the running of the combinations $\tilde{m}_{Q_{33}}^2 + \tilde{m}_2^2$ and $\tilde{A}_{D_{22}} - 2\tilde{A}_{U_{22}}$ are shown, with electroweak and two loop contributions included, in figures (4) and (5) respectively. These QFPs allow us to assess the net effect of electroweak and two-loop contributions; numerically we find

$$\tilde{A}_{U_{\alpha 3}} = \tilde{A}_{U_{3\alpha}} = -0.59$$

$$\begin{aligned}
\frac{6}{5}\tilde{A}_{D_{3\alpha}} - 2\tilde{A}_{U_{ij}} &= 0.49 \\
\tilde{A}_{D_{i\alpha}} - 2\tilde{A}_{U_{ij}} &= 0.60 \\
\tilde{m}_{U_{33}}^2 &= 0.47 \\
\tilde{m}_{Q_{33}}^2 + \tilde{m}_2^2 &= 0.29 \\
\tilde{m}_{Q_{ii}}^2 + 2\tilde{m}_2^2 &= 0.04 \\
\tilde{m}_{U_{ii}}^2 + 2\tilde{m}_2^2 &= -0.01 \\
\tilde{m}_{D_{\alpha\alpha}}^2 + 2\tilde{m}_2^2 &= -0.02 \\
\tilde{m}_1^2 + 2\tilde{m}_2^2 &= -0.72
\end{aligned} \tag{20}$$

which agree well with the analytic approximation. We stress that the analytic and numerical results provide a powerful (and successful) cross check.

These fixed points reveal a remarkable fact for the CMSSM. We have already noted that m_2^2 is driven negative, a requirement of electroweak symmetry breaking. These QFPs tell us that, in the quasi-fixed regime, all the remaining squark mass-squareds are *guaranteed to be positive* at low energy scales, even if their GUT scale values are zero.

Finally in this section, when can we say that we are in the quasi-fixed regime? As a working definition, let us define the quasi-fixed regime to be when \tilde{A}_t varies at the weak scale by less than 5% of its deviation at the GUT scale. Using the solution for \tilde{A}_t with $r = 0.37$, we find that this is true for a remarkably low value; $R_0 \gtrsim 2.5$ or

$$h_t(M_{GUT}) \gtrsim 1.1 \tag{21}$$

This is the case for example in models which, with string theory in mind, take as their Yukawa couplings $h_t = \sqrt{2}g \gtrsim 1.2$ (assuming that renormalisation between the Planck and GUT scales doesn't reduce the Yukawa couplings significantly.)

4 The Spectrum

As well as these QFPs for the specific case of the CMSSM, our solutions quite generally imply a good deal of convergence towards the true fixed points in the infra-red, which we shall refer to as quasi-fixed behaviour. In this section therefore, we return to non-specific patterns of supersymmetry breaking, to consider what this convergence means for the MSSM in general.

Clearly quasi-fixed behaviour indicates that uncertainties in our knowledge of GUT (or Planck) scale physics are less important at low energy. To make this statement quantitative, we introduce a 'focal factor' $F(Y)$ which is defined for some quantity $Y(m_t)$ by the deviation in $Y(m_t)$ produced by independently varying all GUT scale input parameters by 100% of m_g (each deviation being added in quadrature). This value is dependent upon how near one is to the top Yukawa QFP, and here we assign $h_t(M_{GUT}) = 2$ as an example. $F(Y)$ then gives a measure of the dependence of each parameter upon initial conditions³.

³And is also equivalent to the 1σ error in the prediction for $Y(m_t)$ produced by assuming that the GUT scale parameters each have a 1σ deviation of $m_{\tilde{g}}$ around $m_{\tilde{g}}$.

Our prejudice is that the soft supersymmetry breaking terms should all be at least of the same order of magnitude. Accordingly, we choose to determine the spectrum around the central values at the GUT scale;

$$\tilde{m}_{ij}^2 = \tilde{A} = \tilde{B} = 1 \quad (22)$$

In our analytic approximation we find

$$\begin{aligned} -\tilde{A}_U &= \begin{pmatrix} 0.67 & 0.67 & 0.59 \\ 0.67 & 0.67 & 0.59 \\ 0.59 & 0.59 & 0.59 \end{pmatrix} & -\tilde{A}_D &= \begin{pmatrix} 0.75 & 0.75 & 0.75 \\ 0.75 & 0.75 & 0.75 \\ 0.72 & 0.72 & 0.72 \end{pmatrix} \\ \tilde{m}_U^2 &= \begin{pmatrix} 0.90 & 0.14 & 0.08 \\ 0.14 & 0.90 & 0.08 \\ 0.08 & 0.08 & 0.54 \end{pmatrix} & \tilde{m}_D^2 &= \begin{pmatrix} 0.90 & 0.14 & 0.14 \\ 0.14 & 0.90 & 0.14 \\ 0.14 & 0.14 & 0.90 \end{pmatrix} \\ \tilde{m}_Q^2 &= \begin{pmatrix} 0.90 & 0.14 & 0.10 \\ 0.14 & 0.90 & 0.10 \\ 0.10 & 0.10 & 0.72 \end{pmatrix} & \tilde{m}_2^2 &= -0.41 \end{aligned} \quad (23)$$

and the numerical values when all electroweak and two-loop are included are

$$\begin{aligned} -\tilde{A}_U &= \begin{pmatrix} 0.82 & 0.87 & 0.59 \\ 0.82 & 0.97 & 0.59 \\ 0.59 & 0.59 & 0.59 \end{pmatrix} & -\tilde{A}_D &= \begin{pmatrix} 0.96 & 0.96 & 0.96 \\ 0.96 & 0.96 & 0.96 \\ 0.90 & 0.90 & 0.90 \end{pmatrix} \\ \tilde{m}_U^2 &= \begin{pmatrix} 0.91 & 0.14 & 0.07 \\ 0.14 & 0.91 & 0.06 \\ 0.07 & 0.06 & 0.48 \end{pmatrix} & \tilde{m}_D^2 &= \begin{pmatrix} 0.91 & 0.14 & 0.14 \\ 0.14 & 0.91 & 0.14 \\ 0.14 & 0.14 & 0.91 \end{pmatrix} \\ \tilde{m}_Q^2 &= \begin{pmatrix} 0.98 & 0.14 & 0.10 \\ 0.14 & 0.98 & 0.11 \\ 0.10 & 0.11 & 0.75 \end{pmatrix} & \tilde{m}_2^2 &= -0.46 \end{aligned} \quad (24)$$

Since \tilde{B} and $\tilde{\mu}$ are determined by the minimisation of the effective potential they are no longer free parameters. The focal factors are

$$\begin{aligned} F(\tilde{A}_U) &= \begin{pmatrix} .19(.41) & .19(.41) & .02(.39) \\ .19(.41) & .19(.41) & .02(.39) \\ .02(.30) & .02(.30) & .02(.02) \end{pmatrix} & F(\tilde{A}_D) &= \begin{pmatrix} .37(.37) & .37(.37) & .37(.37) \\ .37(.37) & .37(.37) & .37(.37) \\ .31(.37) & .31(.37) & .31(.37) \end{pmatrix} \\ F(\tilde{m}_U^2) &= \begin{pmatrix} .14(.14) & .14(.14) & .08(.08) \\ .14(.14) & .14(.14) & .08(.08) \\ .08(.08) & .08(.08) & .02(.17) \end{pmatrix} & F(\tilde{m}_D^2) &= \begin{pmatrix} .14(.14) & .14(.14) & .14(.14) \\ .14(.14) & .14(.14) & .14(.14) \\ .14(.14) & .14(.14) & .14(.14) \end{pmatrix} \\ F(\tilde{m}_Q^2) &= \begin{pmatrix} .14(.14) & .14(.14) & .11(.11) \\ .14(.14) & .14(.14) & .11(.11) \\ .11(.11) & .11(.11) & .07(.11) \end{pmatrix} & F(\tilde{m}_2^2) &= .08(.11) \end{aligned} \quad (25)$$

where the un-bracketed entries are valid in the CMSSM and the bracketed entries are true for the general (i.e. unconstrained) MSSM.

As an example, let us determine the squark mass-spectrum for these central values, whose values we expect to be close to the real ones (modulo the respective focusing

factors). The mass spectrum depends (to first order) only on A_t through the mixing in the top squark mass matrix. Since \tilde{A}_t always has a QFP, $\tan\beta$ is determined, and μ and B are determined by minimising the effective potential, the entire spectrum depends only on \tilde{m}_{ij}^2 and m_g . Furthermore, the dependence on \tilde{m}_{ij}^2 is also reduced by the infra-red focusing factors above. The minimisation to find μ and B may be done in the same manner as in described in Refs.[9, 5], and yields the mass spectrum for the squarks shown in figure (6), which was determined for negative μ . The masses are almost proportional to m_g (deviation from proportionality coming from M_Z^2 and m_t^2 terms in the mass-squared matrices).

We then expect various models of supersymmetry breaking to give a spectrum close to this one in the quasi-fixed regime (modulo the ‘uncertainty’ represented by the focus factors above). Even allowing for an uncertainty of 100 % in our knowledge of the pattern of supersymmetry breaking at the GUT scale, the focal factors tell us that the mass squareds are determined at the weak scale to better than 14% of m_g^2 . However, note that the off-diagonal elements of the squark mass-squareds \tilde{m}_o^2 are given by $\tilde{m}_o^2 \sim 0.1\tilde{m}_o^2|_0$, and so the quasi-fixed behaviour does not predict the squark mixing, it merely says that it will be fairly small. Thus information about the high-energy physics is retained in the squark sector in the form of the mixings.

Finally, we stress that the improvement in our knowledge of the mass spectrum is due to the existence of *non-zero* true fixed points towards which the soft terms are focusing in the infra-red, and is not simply due to the diverging gluino mass; if all the fixed points had been zero, the squark masses would all have been focused towards zero and, relative to the average squark mass, would have been no better determined than at the GUT scale.

5 Discussion

We now list the assumptions it is necessary to take in order for our analytic solutions in Eq.(11) to be accurate:

- A desert consisting of the MSSM between M_{SUSY} and M_{GUT}
- Low $\tan\beta < 30$, such that h_b and h_τ may be regarded as a small perturbation
- No *large* hierarchies in the soft masses

The last assumption is natural in models of SUSY breaking which have no flavour dependence. A violation of the last assumption may still not be enough to destroy the validity of all of the QFP predictions [10].

There are a number of questions which the quasi-fixed behaviour we have described touch on. First it is striking that just by increasing one parameter h_t we greatly enhance the predictivity of the MSSM especially in the mass spectrum.

Moreover, the soft mass predictions we find are broadly in agreement with electroweak symmetry breaking, and with phenomenology; the m_2^2 term has a negative fixed point to which it is attracted, and in the CMSSM the remaining squark mass-squareds are guaranteed to be positive irrespective of their value at the GUT scale. Perhaps the most interesting and powerful additional constraints may come from the avoidance of charge

and colour breaking minima and potentials which are unbounded from below [12, 13]. In the CMSSM a strong condition comes from the slepton mass squareds [13];

$$m_2^2 + m_L^2 > 0. \quad (26)$$

From our solutions above this translates into $\tilde{m}_1^2 > 0.72$, which, taken at face value, means quite a strong constraint on m_0 ,

$$m_0^2 > 5.5m_{1/2}^2 \quad (27)$$

Whether this and all the other constraints are valid and can be satisfied within the CMSSM will be investigated elsewhere.

Another obvious area of relevance is flavour changing neutral current (FCNC) phenomenology. The focusing behaviour tends to decrease the FCNCs generated from splittings of GUT scale soft masses, supporting previous numerical studies [14]. It is clear however, that the soft parameters do not focus enough to solve the notorious flavour problem associated with the most general supersymmetric breaking. In fact, avoiding too large FCNCs typically implies a constraint on parameters such as

$$\frac{m_s^2 - m_d^2}{m_s^2 + m_d^2}.$$

These are not reduced by the orders of magnitude which would be required for a more general (non-universal) case.

On the other hand we can say something about a picture of CP violation in the MSSM which was proposed recently in Ref.[6], where it was suggested that the CP violation observed in the Kaon system could be solely due to CP violation in the A -terms of the third generation, with the CKM matrix being entirely real. In the quasi-fixed regime, we see that this scenario cannot work when the top Yukawa is at the QFP or very large; the third generation A -terms run to QFPs which are independent of the initial conditions and which do not violate CP. As we have seen this is a quite general property of the MSSM. Thus, deep in the quasi-fixed regime of the MSSM, the only possible source of the observed CP violation is the CKM matrix.

There are many other theoretical and phenomenological aspects of phenomenology where these results will be of relevance. It would be interesting, for example, to calculate what FCNCs the spectrum above predicts. A separate question is whether it is possible to provide similar (but more complicated) analytic solutions for the large $\tan\beta$ regime.

The inverse ('bottom up') approach to that taken in this paper was tried in Ref.[11], where constraints were placed upon GUT scale values from low energy FCNC constraints. However if, as seems likely, h_t is far above its true-fixed point, then the 'bottom up' approach fails (as the authors of Ref.[11] pointed out themselves); a small error in the low energy constraint (such as two loop effects) produces a large error in the GUT scale parameters. Here we see that this is because, in trying to extract information at the GUT scale, one has to fight against the infra-red fixed point structure. So, for example, not only is the prediction for $A_t(M_{GUT})$ derived in Ref.[11] inaccurate for large h_t , but in fact there is no information accessible for $A_t(M_{GUT})$ precisely because it has a QFP.

In summary, we have presented analytic solutions to the RGEs of the soft parameters of the MSSM in the low $\tan\beta$ regime. They are valid when there are no large hierarchies in the soft parameters. The solutions add to our understanding of how the RGEs in

the MSSM act. They exhibit a strong focusing effect: i.e. the low energy parameters are insensitive to their high energy values thus showing quasi-fixed behaviour. The A_t parameter actually has a QFP irrespective of the pattern of supersymmetry breaking, and in the CMSSM there exist other independent QFPs as well. For values of $h_t(M_{GUT}) \gtrsim 1.1$ quasi-fixed behaviour is a dominant feature of the renormalisation group evolution in the MSSM.

6 Acknowledgments

BCA would like to thank the ISN for support, and the ULB for hospitality extended whilst part of this work was being carried out.

References

- [1] B. Pendleton and G.G. Ross, *Phys. Lett.* **B98** (1981) 21; C.T. Hill, *Phys. Rev.* **D24** (1981) 691; B.C. Allanach and S.F. King, RAL-TR-97-019, [hep-ph/9705206](#); B.C. Allanach, G. Amelino-Camelia, O. Philipsen, *Phys. Lett.* **B393** (1997) 349; B.C. Allanach and S.F. King, RAL-97-007, SHEP-97-01 [hep-ph/9703293](#).
- [2] M. Lenzagorta and G.G. Ross, *Phys. Lett.* **B349** (1995) 31; M. Lenzagorta and G.G. Ross, *Phys. Lett.* **B364** (1995) 163.
- [3] B. Schrempp, M. Wimmer, [hep-ph/9606386](#); B. Schrempp, *Phys. Lett.* **B344** (1995) 193.
- [4] H.E. Haber and G.L. Kane, *Phys. Rept.* **117** (1985) 75.
- [5] S.A. Abel, W.N. Cottingham, I.B. Whittingham, *Phys. Lett.* **B370** (1996) 106.
- [6] S.A. Abel, J.M. Frère, *Phys. Rev.* **D55** (1997) 1623.
- [7] P. Langacker and N. Polonsky, *Phys. Rev.* **D52** (1995) 3081.
- [8] S.P. Martin and M.T. Vaughn, *Phys. Rev. D* **50** (1994) 2282.
- [9] V. Barger, M.S. Berger and P. Ohmann, *Phys. Rev.* **D49** (1994) 4908; G.L. Kane, C. Kolda, L. Roszkowski *et al*, *Phys. Rev.* **D49** (1994) 6173.
- [10] S.A. Abel and B.C. Allanach, work in progress.
- [11] M. Carena, P. Chankowski, M. Olechowski, S. Pokorski and C.E.M. Wagner, *Nucl. Phys.* **B491** (1997) 103
- [12] H.-P. Nilles, M. Srednicki and D. Wyler, *Phys. Lett.* **B120** (1983) 346; J.-M. Frère, D.R.T. Jones and S. Raby, *Nucl. Phys.* **B222** (1983) 11; J.-P. Derendinger and C.A. Savoy, *Nucl. Phys.* **B237** (1984) 307; C. Kounnas, A.B. Lahanas, D.V. Nanopoulos and M. Quirós, *Nucl. Phys.* **B236** (1984) 438; M. Drees, M. Glück and K. Grassie, *Phys. Lett.* **B157** (1985) 164; J.F. Gunion, H.E. Haber and M. Sher,

Nucl. Phys. **B306** (1988) 1; P. Langacker and N. Polonsky, *Phys. Rev.* **D50** (1994) 2199; J.A. Casas and S. Dimopoulos, *Phys. Lett.* **B387** (1996) 107; J.A. Casas, A. Lleyda and C. Muñoz, *Phys. Lett.* **B389** (1996) 305.

[13] H. Komatsu, *Phys. Lett.* **B215** (1988) 323.

[14] D. Choudhury, F. Eberlein, A. König, J. Louis, S. Pokorski, *Phys. Lett.* **B342** (1995) 180.

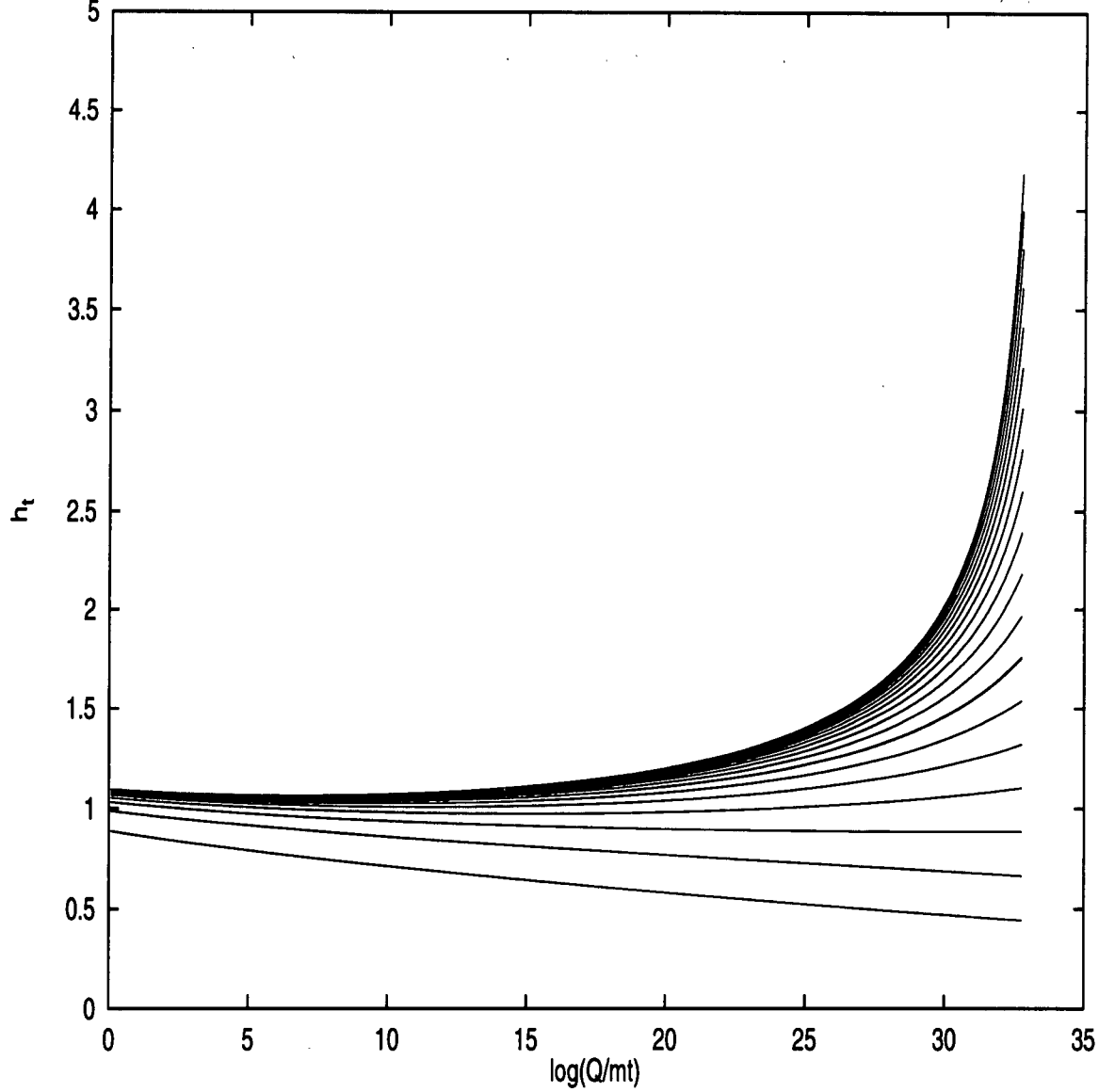


Figure 1: The two-loop renormalisation of the top Yukawa coupling, h_t , for $m_t = 140$ GeV. We have included electroweak and h_b, h_τ corrections and $\tan \beta$ is determined separately for each line by Eq.(1). The true fixed point is $h_t/g_3 = 0.9$ and is invariant under the renormalisation group. Electroweak corrections make this higher than the naive value, $h_t = \sqrt{7/18}g_3$. The formal quasi-fixed point is the curve for which $h_t(GUT) = \infty$.

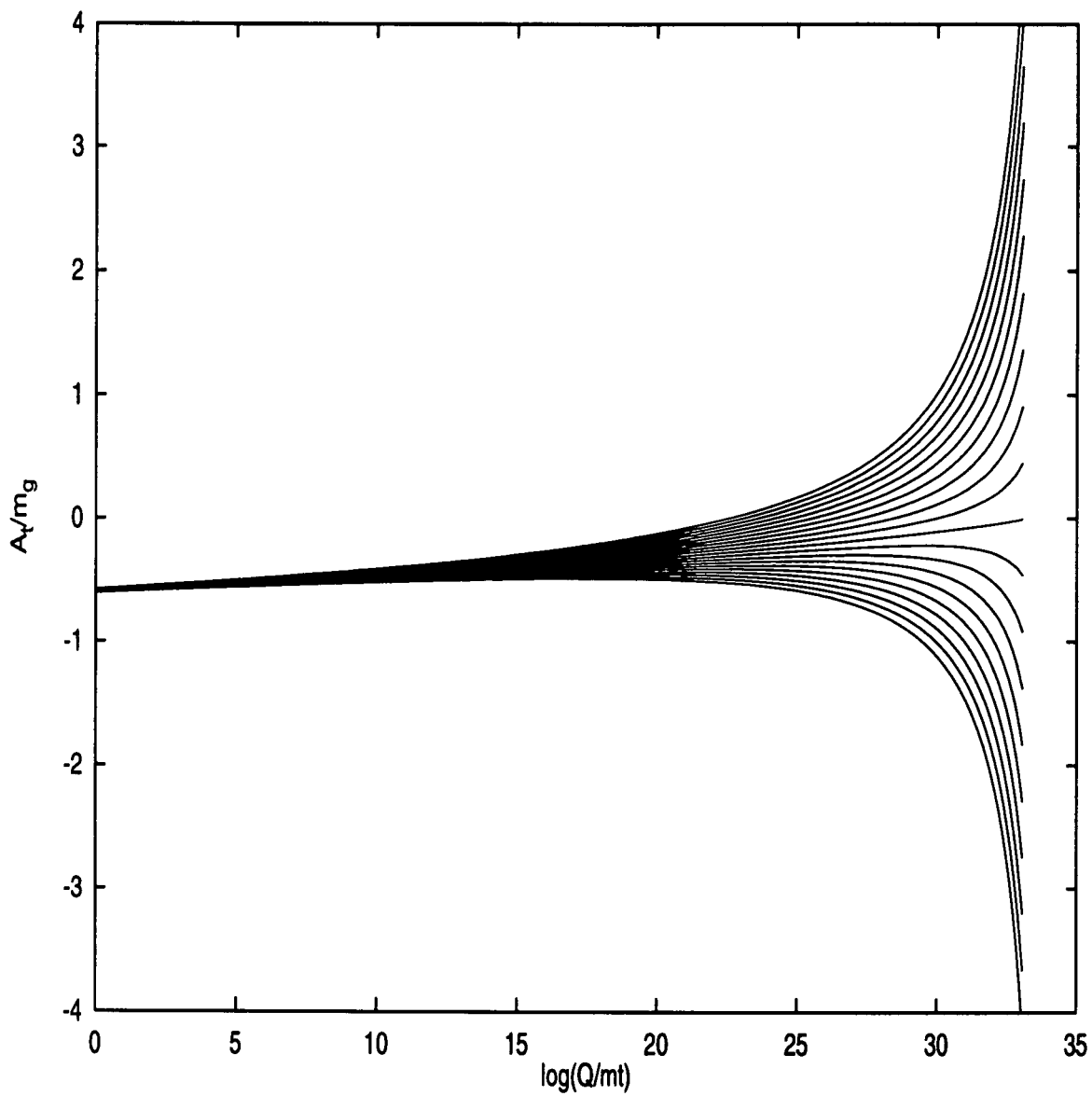


Figure 2: Two-loop renormalisation of A_t/m_g in the CMSSM for various different initial values, with $h_t(GUT) = 5g_3(GUT)$ and $m_t = 175$ GeV. All electroweak and Yukawa contributions are included.

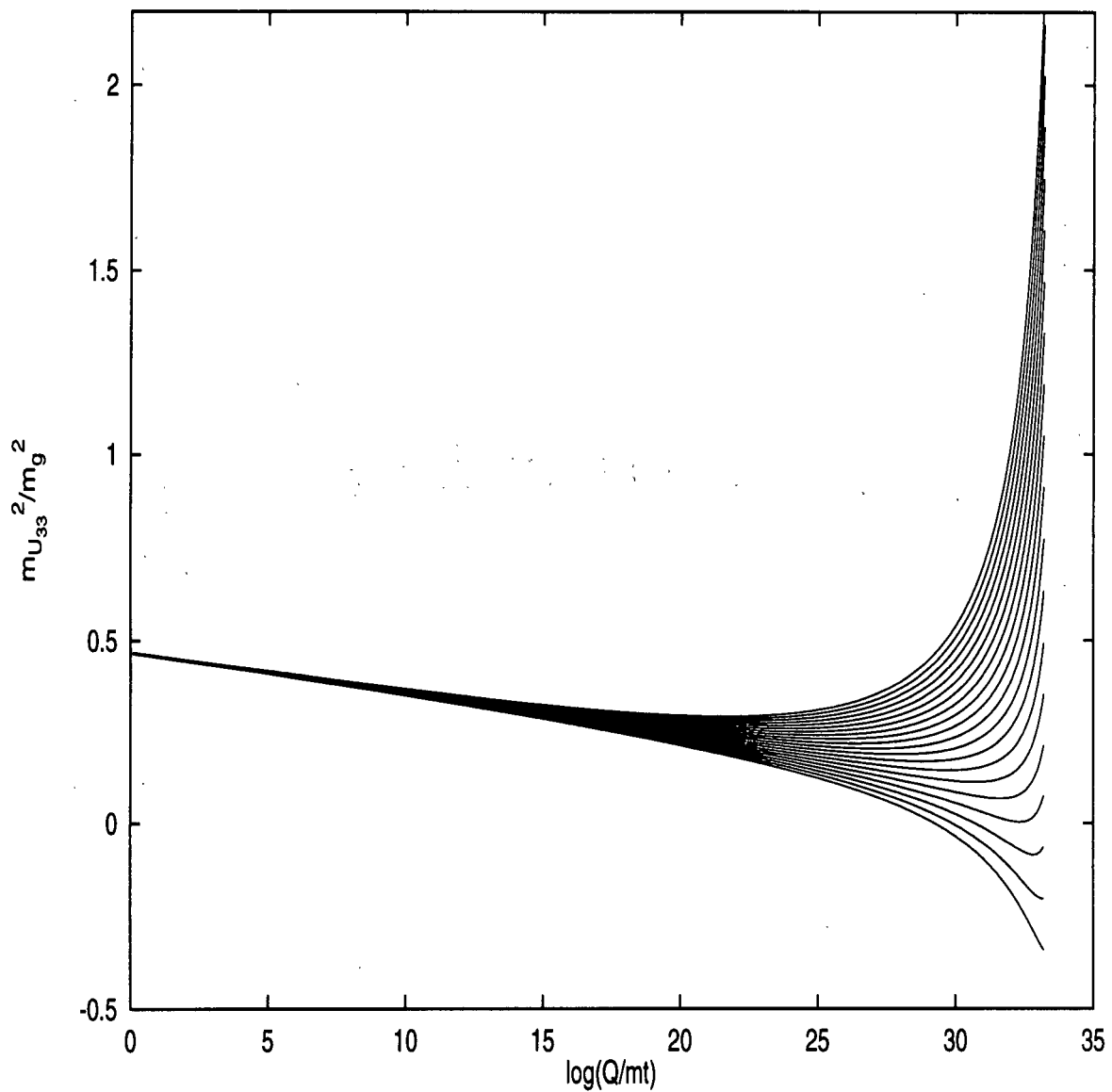


Figure 3: Two-loop renormalisation of $m_{U_{33}}^2/m_g^2$ in the CMSSM, with $h_t(GUT) = 5g_3(GUT)$ and $m_t = 175$ GeV. All electroweak and Yukawa contributions are included.

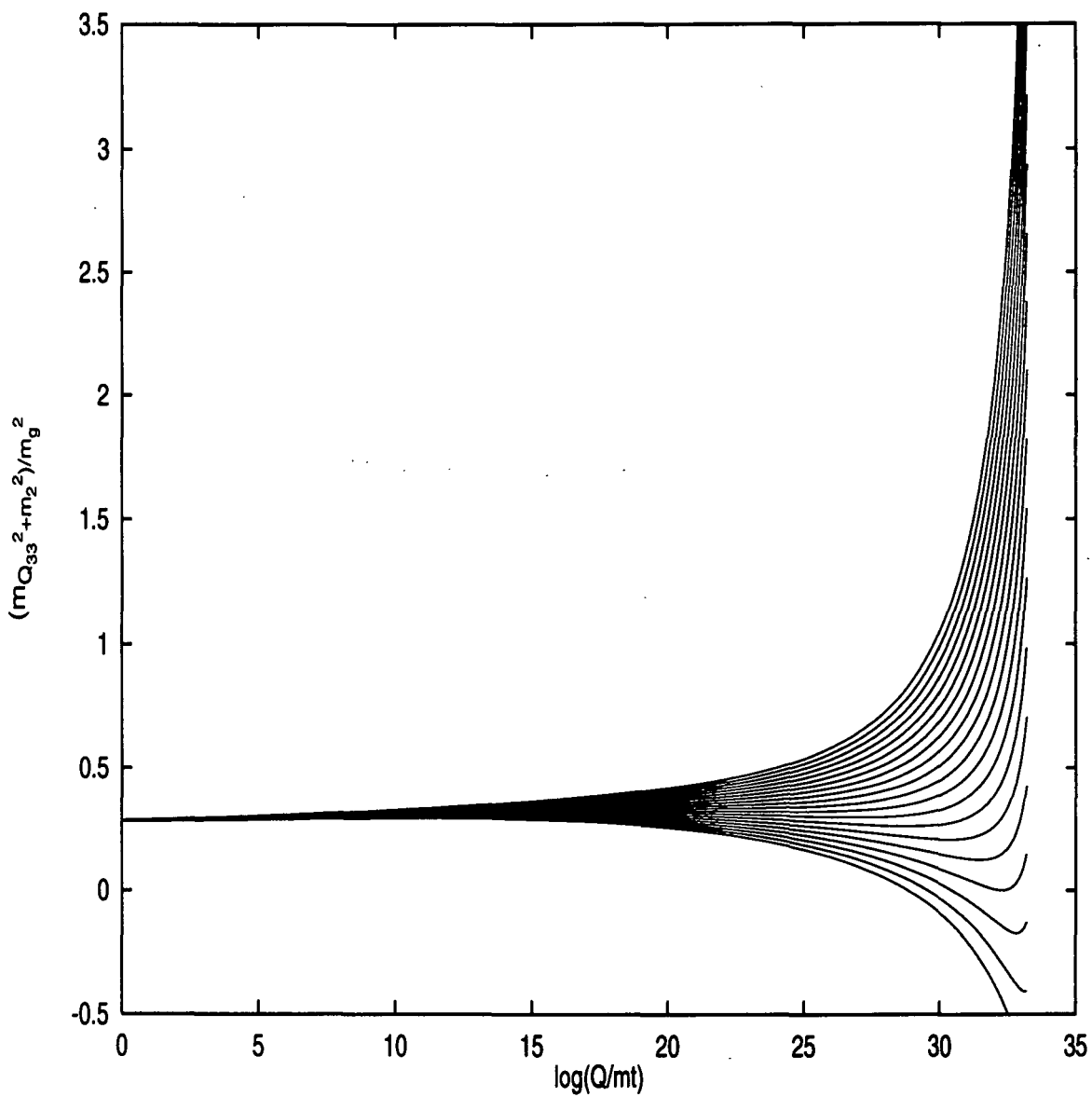


Figure 4: Two-loop renormalisation of $(m_{Q_{33}}^2 + m_2^2)/m_g^2$ in the CMSSM, with $h_t(GUT) = 5g_3(GUT)$ and $m_t = 175$ GeV. All electroweak and Yukawa contributions are included.

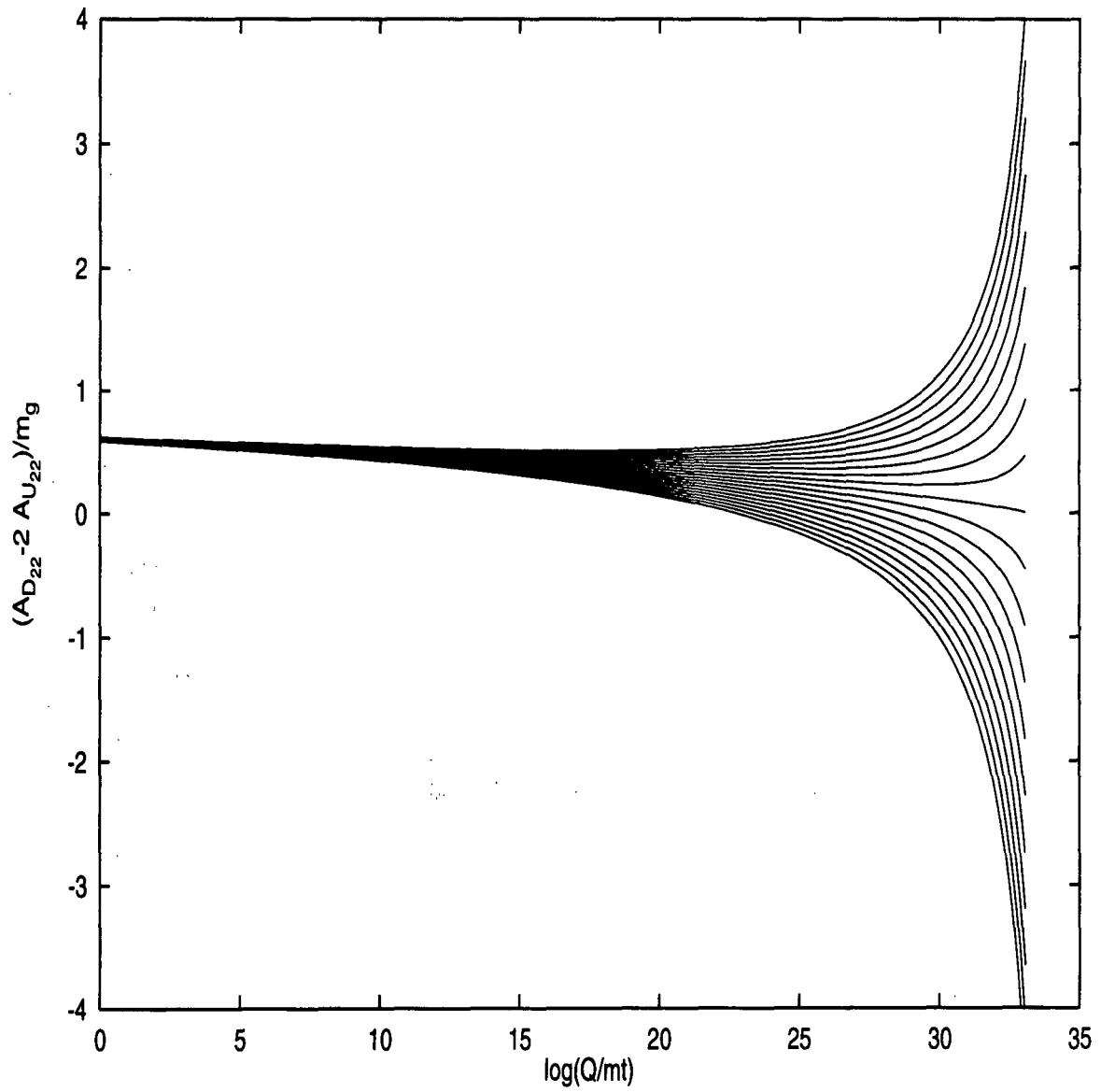


Figure 5: Two-loop renormalisation of $(\tilde{A}_{D_{22}} - 2\tilde{A}_{U_{12}})/m_g$ in the CMSSM, with $h_t(GUT) = 5g_3(GUT)$ and $m_t = 175$ GeV in the CMSSM. All electroweak and Yukawa contributions are included.

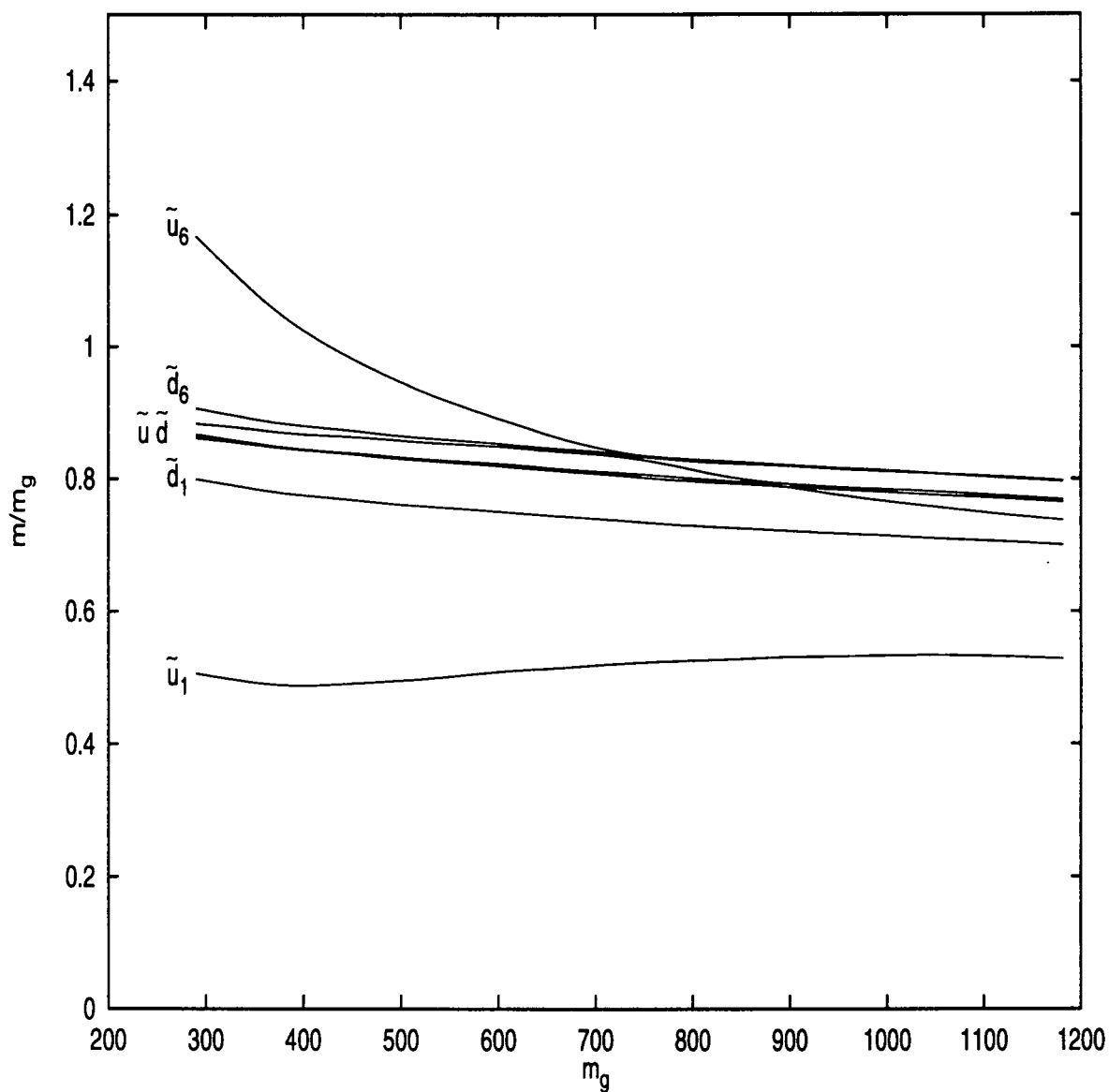


Figure 6: Mass spectrum of the squarks when $h_t(GUT) = 2$ and $m_t = 175$ GeV as a function of m_g in the CMSSM. All electroweak and Yukawa contributions are included. An error of $\pm m_g$ at the GUT scale, corresponds to ± 0.18 in this spectrum.